Subject-Specific Modeling of Human Ribs: Finite Element Simulations of Rib Bending Tests, Mesh Sensitivity, Model Prediction with Data Derived From Coupon Tests

Keegan Yates, Costin Untaroiu
Virginia Tech, Blacksburg, VA, USA

Abstract

Rib fractures are common thoracic injuries in motor vehicle crashes. The main objective of this study was to investigate the predictability of subject specific rib models under bending loading. The exterior geometries of two human ribs as well as the boundaries between the trabecular and cortical layers were extracted from corresponding CT-images. Then, the mesh of one rib was developed in a parametric fashion. To investigate the mesh influence on the model response, three models with solid elements (1, 2, 3 elements into rib thickness) and one with shell elements with non-uniform thickness (extracted from CT-images) were developed. The meshes of other rib (4 models for each rib) were obtained using an in-house morphing program specially developed for ribs. Briefly, this algorithm used an automated landmark-based approach to define both the outer and inner boundaries of the cortical layer. The landmarks were then used in a thin plate spline warping algorithm to warp the template nodes to the target geometry. The material and failure properties of the rib models were defined based on the stress-strain data obtained from coupon tests at Virginia Tech (VT) for each rib. Full rib impacts were simulated in LS-DYNA® based on data recorded in testing at Ohio State University (OSU). The force and strain time histories recorded in testing were compared with corresponding FE data. Overall, the results showed similar trends as test data, but some sensitivity relative to the modeling approach was observed. For example, shell models showed a stiffer response than solid models, and single element cortical layer models were softer than two or three layer models. Additionally, although failure was defined in the material model, none of the models experience fractures during the FE simulations. This highlights the need for better algorithms to determine cortical thickness as well as material models to account for the anisotropy of bone.

Introduction

Understanding the mechanisms leading to rib fractures is an important challenge for engineers and vehicle safety researchers, as injuries to the thorax can rapidly become life threatening. Computational models of the entire human, including the thorax, have been created, usually based on the geometries of a certain volunteer subject's anatomical structures [1-4]. However, these models have some limitations related to possible inaccuracies from the thickness estimation of cortical bone [5] and the material properties assigned based on literature data. These inaccuracies correlated with the rib dependency on various modeling approaches make it challenging to interpret the responses predicted by current human rib models [6, 7]. To address these challenges, considerable experimental effort has been made on a variety of scales to better understand rib impact response, from rib cortical coupon testing [8] to individual rib testing [7, 9, 10] to testing of intact thoraces [11]. Additionally, many computational approaches have supplemented experimental tests, including single rib [12] and full body [1, 2] finite element modeling as well as morphometric/parametric modeling of the rib cage [13-15].

The current study tries to provide a better understanding of the FE rib model responses under bending loading by utilizing automated mesh morphing techniques to rapidly create new models.

Methods

A segmentation procedure was performed in MIMICS software (v19, Materialise, Leuven, Belgium) to reconstruct the interior and exterior surfaces of rib cortical bone of two ribs tested under bending loading at Ohio State University [7]. The HU threshold range for cortical bone suggested by the MIMICS software (662-1988) were initially used to distinguish the cortical bone from CT images. Then, each rib slice was reviewed

and some manual changes were performed especially in the cross-section where some discontinuity in the bone was observed. Finally, both the external and internal (cortical-trabecular boundary) surfaces of the ribs were exported in IGES format and used to develop the rib mesh. The mesh of one rib model was generated using TrueGrid (XYZ Scientific Applications, Livermore, CA), which utilizes a structural approach to mesh complex three-dimensional objects using exclusively hexahedral solid elements. This method had the advantage that it is script driven and parametric. Therefore, refining the mesh based on the original geometry, and using updated surfaces of the geometry became trivial. To investigate the influence of different meshes on the rib model response, four FE models were generated: a) three solid models with 1, 2, or 3 elements through the rib thickness (Fig. 1abc) and b) one shell model (Fig. 1d) with the cortical bone thickness calculated automatically and defined at each shell node by an in-house software. As shown in figure 1, the interior of the rib models was filled with solid elements assigned with the material properties of trabecular bone.
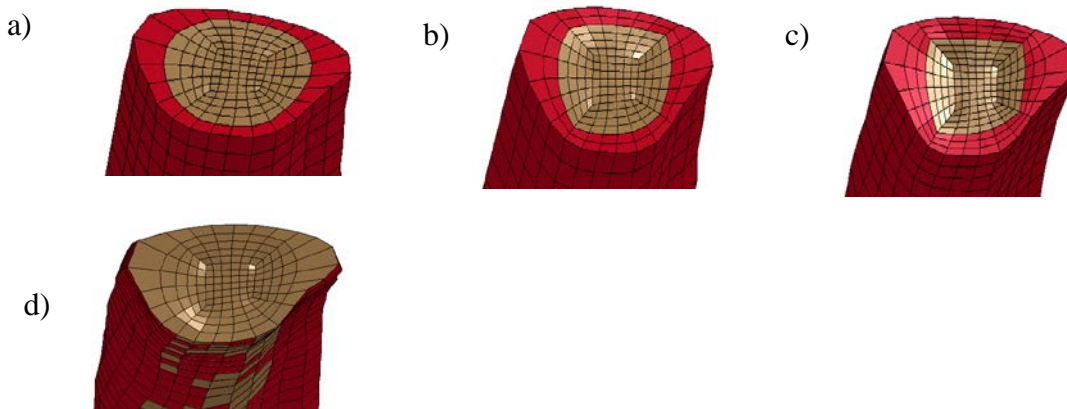
Figure 1. FE meshing of human rib using solid 1 (a), 2 (b), and 3 (c) elements for cortical bone and using shell elements for cortical bone (d).

To create meshes of additional ribs, a morphing program was developed in Matlab (Mathworks, Natick, MA). This morphing approach creates new rib meshes with an equal number of nodes and elements, and similar element quality. Corresponding landmarks on each rib were determined using an automated shape analysis procedure. Briefly, point clouds were obtained from the inside and outside of the segmented cortical layer (Fig 2a). Next, these point clouds were aligned with the point clouds from the original template rib, and corresponding landmarks were found on the outer surface of the rib, as well as the border between the cortical and trabecular layers.
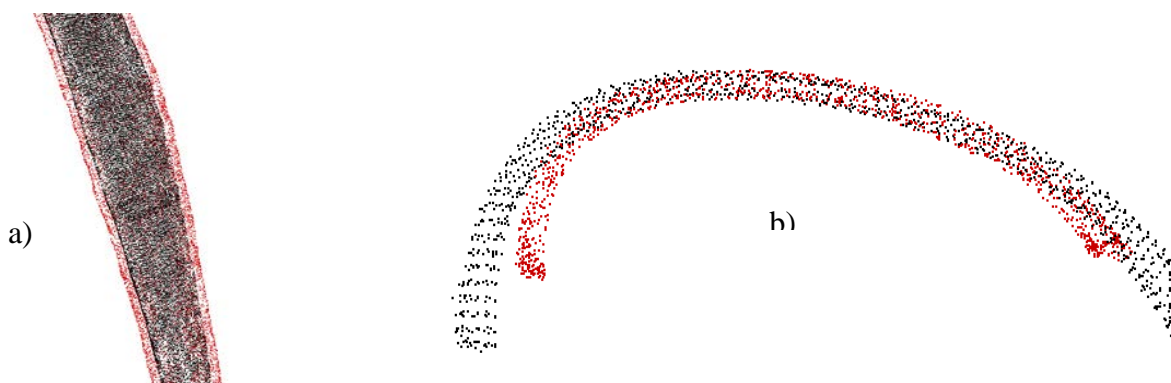

Fig. 2. Point clouds (a) from inside (black) and outside (red) of cortical layer. Landmarks (b) from template rib (black) and target rib (red) used for mesh morphing.

The landmark finding algorithm is further explained in Yates et al. [16] Rather than using several dozen manually identifiable landmarks located only on the surface of the rib, this allowed for over 1,000 landmarks to

characterize each rib, including the variation of cortical thickness throughout the rib (Fig. 2b). Next, these landmarks were used in conjunction with a thin plate spline warping procedure [17] to warp the template rib nodes to the target geometry. This process was used for the one, two, and three cortical element thickness meshes. Meshes with a layer of cortical shell elements were created from the one element mesh by finding the thickness at each cortical node, and projecting it into shell elements with nodal thicknesses[4].

The OSU testing set-up simulated a dynamic frontal impact in which the sternal end of the rib was pushed towards the vertebral end to create a 2D bending scenario (Fig. 3). A 54.4 kg pendulum impacted the potted sternal end of the ribs along the x-axis, the primary loading direction [7]. The ribs were free to rotate around the center of each potted end. The time history of the sternal rib end (moving part) was measured using a linear string potentiometer and was used as input in FE simulation. The forces and moments were recorded by a 6-axis load cell behind the fixed end. The time history of x-axis force recorded in testing was compared with the corresponding force calculated during FE simulation. Strain gauges were positioned on the pleural and cutaneous surfaces at 30% (SG1) and 60% (SG2) of the curve length of the potted rib from vertebral to sternal end. To calculate the strain time histories during the FE simulation, shell elements were defined at approximated location of test strain gages reported in testing. The characteristics of the PMHS's and ribs used in this study are shown in table 1.
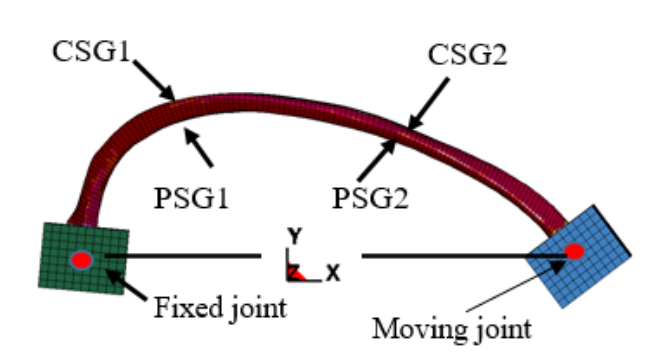

Figure 3. FE model of experimental setup.

Table 1. The characteristics of the modelled ribs presented in this study

Rib number	PMHS			Rib	
	Height (cm)	Weight (kg)	Sex/Age	Type	Span (mm)
1	191	75	M/59	Left 6th	237
2	168	60	M/59	Right 6th	214

An elastic-plastic material model (MAT_24, LS-DYNA) was used for cortical bone in both rib models. The bilinear curves of each rib material model (Fig. 4) were defined based on stress-strain curves obtained from tensile coupon tests at VT [18]. The parameters of each rib material model are presented in Table 2. The trabecular bone was modeled using the same elastic-plastic material model for both rib models.
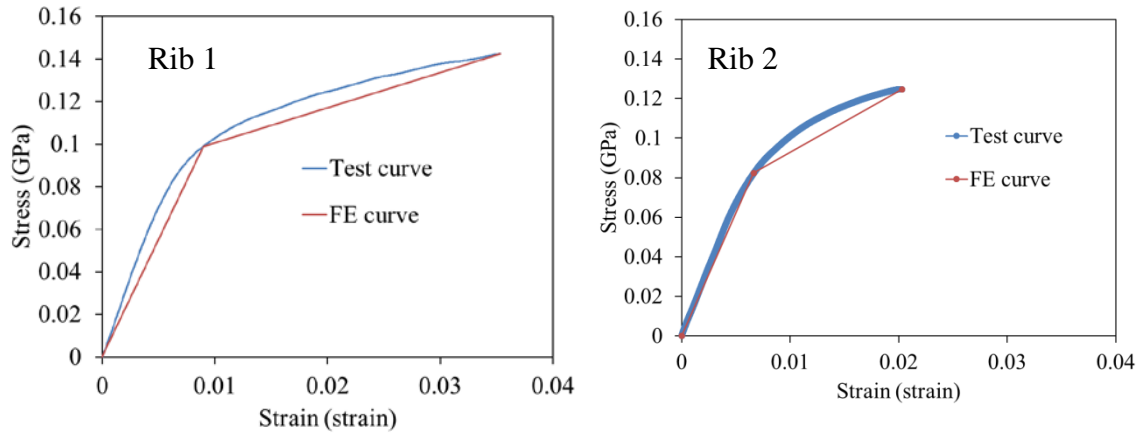
Fig. 4. The stress-strain curves obtained from tensile coupon tests vs. corresponding curves defined in the cortical bone rib model.

Table 2. The material parameters of rib cortical/trabecular bone

Rib number		Young's modulus (GPa)	Tangent modulus (GPa)	Yield stress (MPa)	Failure plastic strain (%)
1	Cortical	11.03	1.645	98.98	2.635
2		12.38	9.38	82.36	1.367
Both	Trabecular	0.04	0.001	1.8	2.00

The integration formulation for solid elements was assigned as constant stress solid element (1-point integration) and an hourglass control (Type 4, Flanagan-Belytschko stiffness form) was used to reduce hourglass energy (QM= 0.005). The integration formulation for shell elements was assigned as Belytschko-Tsay with 2 integration points through thickness. The same hourglass control approach used in solid elements was used in the shell elements as well.

Results

The time histories force along the loading axis (x-direction) recorded in testing were compared with the corresponding data predicted by rib FE models (Fig. 5). As shown, the responses of FE models are dependent on the modeling approach used. The rib solid models predict a softer response than the rib shell models. The solid models with 1 element in thickness have a softer response than the rib models with 2 or 3 elements in the thickness of rib cortical bone.
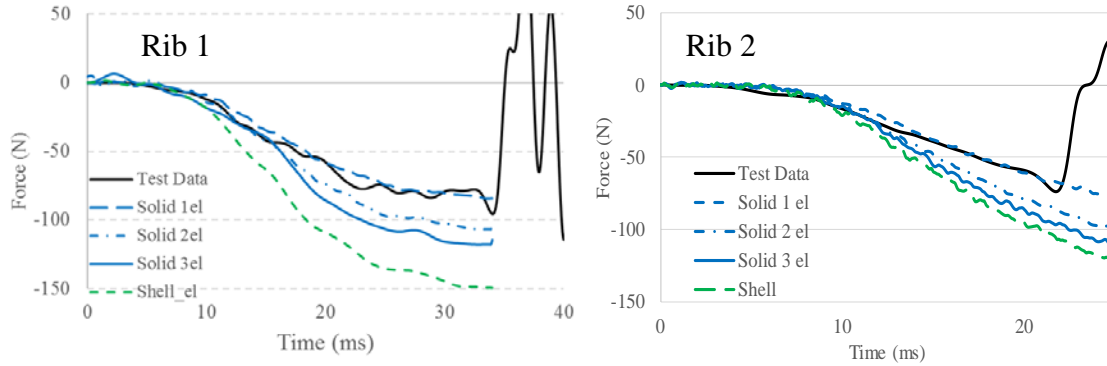
Fig. 5. The force time histories of the FE simulations vs. the test data.

The strain response predicted by each FE model was compared to the corresponding test data for ribs 1 and 2 (Figs 6, 7). As shown, the strain response predicted by FE models showed the same polarity, but the closeness to the test data depends on the rib and strain gage location. For example, CSG 1 and 2 data (in tension) was usually closer to the test data compared to similar data predicted by PSG 1 and 2 (in compression). Finally, it should be mentioned that no fractures were observed in all simulations even though the fracture option was turned on with the thresholds determined from coupon tests.
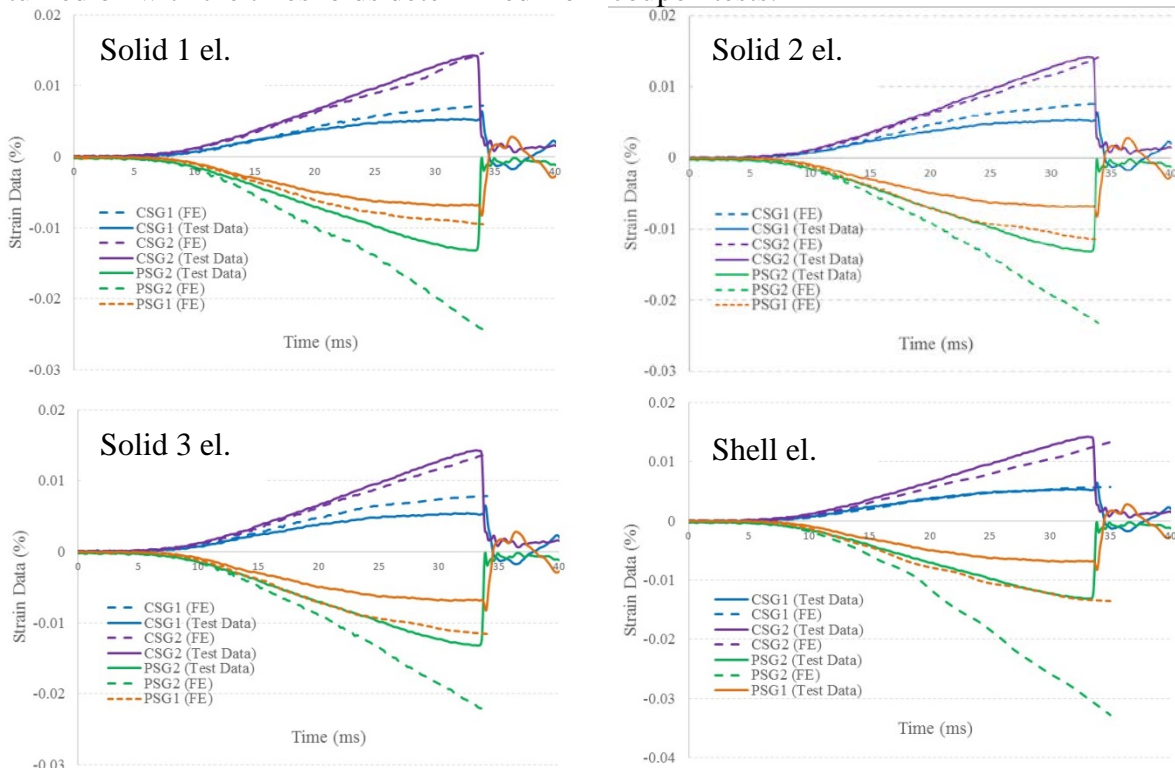
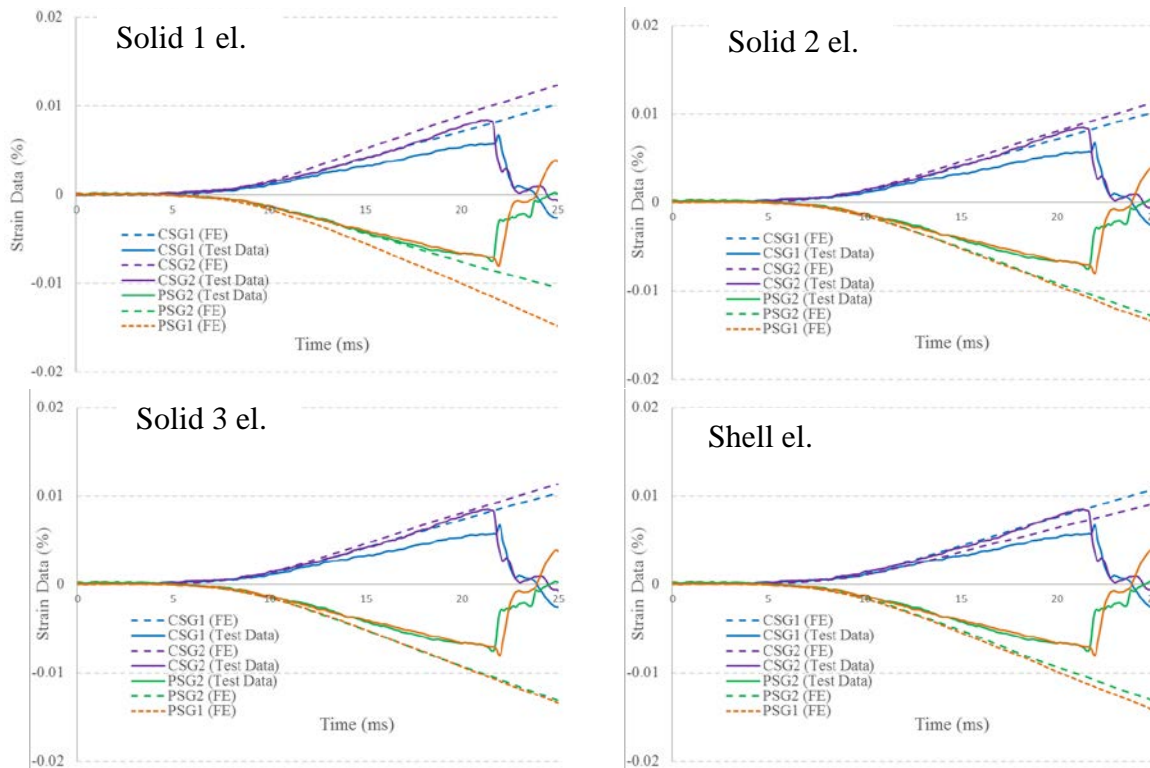**Fig. 6**. Comparison of strain data. Test vs. FE models (Rib 1).

Fig. 7. Comparison of strain data. Test vs. FE models (Rib 2).

Conclusions

Two rib tests were modeled in this study to investigate the predictability of FE models relative to test data in terms of global (force) and local (strain) responses under bending loading. The rib geometries were reconstructed from clinical CT-images and four models were generated for both ribs. The material models of each rib were defined based on the tensile stress-strain curves obtained from coupon test of the corresponding rib. Both global and local responses showed the same trends as test data. However, some differences were observed between the models generated using the same geometry and material properties. The rib shell models were always stiffer than the rib solid models and test data. The differences between the rib models and test data could be also caused by inaccuracies from identification of rib geometry from clinical CT-images and complex properties of cortical bone (anisotropy, inhomogeneity, viscoelasticity, different behavior in tension/compression, etc.). While only two ribs were modeled in this study and it is known that inter-personal variability play a significant role in mechanical behavior of human ribs, modeling more specimens are suggested for future in order to derive stronger conclusions. These models could be rapidly developed with the aid of the morphing algorithm. In future models, a better approach for the reconstruction of rib geometry is suggested. For example, in addition to MIMICS software, it is suggested to use new software packages developed for better estimation of cortical thickness [19] (e.g. Stradwin, v.5.0, Cambridge, England). The data obtained could be validated based on the micro-CT data provided by OSU for certain regions. In addition to the homogenous material models used in this study (MAT-24), the performance of other LS-DYNA models could be evaluated. Optimization techniques could also be used to find the most appropriate material parameters for a certain rib model.

Acknowledgement

References

[1]   M. Iwamoto, Y. Nakahira, and H. Kimpara, "Development and Validation of the Total HUman Model for Safety (THUMS) Toward Further Understanding of Occupant Injury Mechanisms in Precrash and During Crash," *Traffic Inj Prev,* vol. 16 Suppl 1, pp. S36-48, 2015.

[2]   N. A. Vavalle, D. P. Moreno, A. C. Rhyne, J. D. Stitzel, and F. S. Gayzik, "Lateral impact validation of a geometrically accurate full body finite element model for blunt injury prediction," *Ann Biomed Eng,* vol. 41, no. 3, pp. 497-512, Mar 2013.

[3]   N. Yue and C. D. Untaroiu, "A numerical investigation on the variation in hip injury tolerance with occupant posture during frontal collisions," *Traffic Inj Prev,* vol. 15, no. 5, pp. 513-22, 2014.

[4]   C. D. Untaroiu, N. Yue, and J. Shin, "A finite element model of the lower limb for simulating automotive impacts," *Ann Biomed Eng,* vol. 41, no. 3, pp. 513-26, Mar 2013.

[5]   R. Perz, J. Toczyski, and D. Subit, "Variation in the human ribs geometrical properties and mechanical response based on X-ray computed tomography images resolution," *J Mech Behav Biomed Mater,* vol. 41, pp. 292-301, Jan 2015.

[6]   J. L. Forman, R. W. Kent, K. Mroz, B. Pipkorn, O. Bostrom, and M. Segui-Gomez, "Predicting rib fracture risk with whole-body finite element models: development and preliminary evaluation of a probabilistic analytical framework," in *Annals of Advances in Automotive Medicine/Annual Scientific Conference*, 2012, vol. 56, p. 109: Association for the Advancement of Automotive Medicine.

[7]   A. M. Agnew, M. Schafman, K. Moorhouse, S. E. White, and Y. S. Kang, "The effect of age on the structural properties of human ribs," *J Mech Behav Biomed Mater,* vol. 41, pp. 302-14, Jan 2015.

[8]   A. R. Kemper *et al.*, "Material properties of human rib cortical bone from dynamic tension coupon testing," SAE Technical Paper2005.

[9]   M. M. Murach *et al.*, "Rib Geometry Explains Variation in Dynamic Structural Response: Potential Implications for Frontal Impact Fracture Risk," *Ann Biomed Eng,* vol. 45, no. 9, pp. 2159-2173, Sep 2017.

[10]   M. A. Schafman, Y. S. Kang, K. Moorhouse, S. E. White, J. H. t. Bolte, and A. M. Agnew, "Age and sex alone are insufficient to predict human rib structural response to dynamic A-P loading," *J Biomech,* vol. 49, no. 14, pp. 3516-3522, Oct 3 2016.

[11]   C. K. Kroell, D. C. Schneider, and A. M. Nahum, "Impact tolerance and response of the human thorax II," SAE Technical Paper0148-7191, 1974.

[12]   Z. Li *et al.*, "Rib fractures under anterior–posterior dynamic loads: experimental and finite-element study," *Journal of biomechanics,* vol. 43, no. 2, pp. 228-234, 2010.

[13]   X. Shi, L. Cao, M. P. Reed, J. D. Rupp, C. N. Hoff, and J. Hu, "A statistical human rib cage geometry model accounting for variations by age, sex, stature and body mass index," *J Biomech,* vol. 47, no. 10, pp. 2277-85, Jul 18 2014.

[14]   Y. Wang *et al.*, "A parametric ribcage geometry model accounting for variations among the adult population," *J Biomech,* vol. 49, no. 13, pp. 2791-2798, Sep 6 2016.

[15]   A. A. Weaver, S. L. Schoell, and J. D. Stitzel, "Morphometric analysis of variation in the ribs with age and sex," *J Anat,* vol. 225, no. 2, pp. 246-61, Aug 2014.

[16]   K. M. Yates, Y. C. Lu, and C. D. Untaroiu, "Statistical shape analysis of the human spleen geometry for probabilistic occupant models," *J Biomech,* vol. 49, no. 9, pp. 1540-6, Jun 14 2016.

[17]   F. L. Bookstein, "Information Processing in Medical Imaging," in *Thin-Plate splines and the atlas problem for biomedical images*, A. C. F. Colchester, Hawkes, D. J., Ed. Berlin Heidelberg: Springer, 1991, pp. 326-342.

[18]   D. L. Albert, Y.-S. Kang, A. M. Agnew, and A. R. Kemper, "A Comparison of Rib Structural and Material Properties from Matched Whole Rib Bending and Tension Coupon Tests," in *IRCOBI Conference Proceedings*, 2017.

[19]   C. Okoukoni *et al.*, "Early dose-dependent cortical thinning of the femoral neck in anal cancer patients treated with pelvic radiation therapy," *Bone,* vol. 94, pp. 84-89, Jan 2017.